New Tellurites: Syntheses, Structures, and Characterization of $K_2Te_4O_9 \cdot 3.2H_2O$, $KGaTe_6O_{14}$, and $KGaTe_2O_6 \cdot 1.8H_2O$

Kang Min Ok and P. Shiv Halasyamani*

Department of Chemistry, University of Houston, 4800 Calhoun Blvd., Houston, Texas 77204-5003

Received April 23, 2001. Revised Manuscript Received August 8, 2001

Single crystals of $K_2Te_4O_9 \cdot 3.2H_2O$, $KGaTe_6O_{14}$, and $KGaTe_2O_6 \cdot 1.8H_2O$ have been synthesized by supercritical hydrothermal methods using KOH, TeO_2, and Ga_2O_3 as reagents. $K_2Te_4O_9 \cdot 3.2H_2O$ has a layered structure, whereas $KGaTe_6O_{14}$ and $KGaTe_2O_6 \cdot 1.8H_2O$ have three-dimensional frameworks. In addition, $KGaTe_2O_6 \cdot 1.8H_2O$ has an unprecedented open-framework tellurite topology that permits the ion exchange of Li^+ and Na^+. In addition, the ion-exchanged phases are highly crystalline. Crystal data: $K_2Te_4O_9 \cdot 3.2H_2O$, triclinic, space group $P1$ (No. 1), with $a = 7.5046(5)$ Å, $b = 10.7097(8)$ Å, $c = 10.7159(8)$ Å, $\alpha = 60.849(1)°$, $\beta = 69.918(1)°$, $\gamma = 85.968(1)°$, and $Z = 2$; $KGaTe_6O_{14}$, cubic, space group Pa-3 (No. 205), with $a = 10.9267(3)$ Å and $Z = 4$; $KGaTe_2O_6 \cdot 1.8H_2O$, triclinic, P-1 (No. 2), with $a = 8.8361(6)$ Å, $b = 9.1648(6)$ Å, $c = 9.9531(7)$ Å, $\alpha = 115.395(1)°$, $\beta = 93.973(1)°$, $\gamma = 116.011(1)°$, and $Z = 3$.

Introduction

Owing to their widespread application in catalysis, energy storage, sorption, and ion exchange, open-framework materials are of great interest.[1,2] A specific class of these materials are zeolites (aluminosilicates). Because of their industrially important physical properties,[3] a great deal of effort has been expended to understand their syntheses and structures. A related research area concerns synthesizing new non-aluminosilicate zeolitic materials. Beginning with the aluminum phosphates, i.e., AlPO's,[4] this chemistry has been extended to encompass a variety of elements.[5−9] Despite these efforts, open-framework tellurites (Te^{4+}) are extremely rare. In fact, only one naturally occurring open-framework tellurite mineral, Zemannite $Mg_{0.5}[(Zn,Fe)_2(TeO_3)_3] \cdot 4.5H_2O$,[10−12] has been found, and although selenites isostructural to Zemannite have been reported,[13] only one instance of synthetic Zemannite has been reported.[14] We recently reported the synthesis and structure of $NaGaTe_2O_6 \cdot 2.4H_2O$,[15] an open-framework tellurite with a Zemannite-like structure.

We are interested in exploring the synthesis of tellurites for a number of reasons. First, a variety of structural motifs are possible for tellurites. Tellurium polyhedral connectivity range from fully bonding, e.g., $[TeO_{4/2}]^0$ and $[TeO_{3/2}]^+$, to completely terminal, e.g., $[TeO_{3/1}]^{2-}$.[16,17] This variable coordination geometry combined with octahedral or tetrahedral moieties suggests that a great deal of flexibility in any framework architecture is possible and, furthermore, indicates the potential for a variety of open-framework topologies. Second, as with Zemannite and $NaGaTe_2O_6 \cdot 2.4H_2O$, reversible hydration properties are possible. Finally, as we will show in this article, open-framework tellurites are extremely amenable to the ion exchange of a variety of cations. Previously, tellurites have been synthesized by solid state,[17−20] solution,[21,22] and supercritical hydrothermal techniques.[23−26] The latter method has been used extensively by Kolis et al. in the synthesis of a variety of mixed metal tellurites and tellurium oxychlorides.[23−26] The use of supercritical hydrothermal techniques to synthesize new materials is well docu-

* To whom correspondence should be addressed.

(1) Davis, M. E.; Lobo, R. F. *Chem. Mater.* **1992**, *4*, 756.
(2) Francis, R. F.; O'Hare, D. *J. Chem. Soc., Dalton Trans.* **1998**, 3133.
(3) Venuto, P. B. *Microporous Mater.* **1994**, *2*, 297.
(4) Estermann, M.; McCuster, L. B.; Baerlocher, C.; Merrouche, A.; Kessler, H. *Nature* **1991**, *352*, 320.
(5) Hausalter, R. C.; Mundi, L. A. *Chem. Mater.* **1992**, *4*, 31.
(6) Cavellec, M.; Riuo, D.; Ninclaus, C.; Greneche, J. M.; Ferey, G. *Zeolites* **1996**, *17*, 250.
(7) Chippindale, A. M.; Brech, S. J.; Cowly, A. R.; Simpson, W. M. *Chem. Mater.* **1996**, *8*, 2259.
(8) Ayyappan, S.; Cheetham, A. K.; Natarajan, S.; Rao, C. N. R. *J. Solid State Chem.* **1998**, *139*, 207.
(9) Halasyamani, P. S.; Walker, S. M.; O'Hare, D. *J. Am. Chem. Soc.* **1999**, *121*, 7415.
(10) Zemann, J. Z. *Z. Kristallogr.* **1968**, *127*, 319.
(11) Mandarino, J.; Matzat, E.; Williams, S. J. *Can. Miner.* **1976**, *14*, 387.
(12) Miletich, R. *Euro. J. Miner.* **1995**, *7*, 509.
(13) Wildner, M. *Mineral. Petrol.* **1993**, *48*, 215.
(14) Miletich, R. *Monatsh. fur Chem.* **1995**, *126*, 417.
(15) Bhuvanesh, N. S. P.; Halasyamani, P. S. *Inorg. Chem.* **2001**, *40*, 1404.
(16) Tatsumisago, M.; Minami, T.; Kowada, Y.; Adachi, H. *Phys. Chem. Glasses* **1994**, *35*, 89.
(17) Becker, C. R.; Tagg, S. L.; Huffman, J. C.; Zwanziger, J. W. *Inorg. Chem.* **1997**, *36*, 5559.
(18) Hanke, K.; Kupcik, V. *Acta Crystallogr.* **1973**, *B29*, 963.
(19) Johansson, G. B.; Lindqvist, O. *Acta Crystallogr.* **1978**, *B34*, 2959.
(20) Platte, C.; Tromel, M. *Acta Crystallogr.* **1981**, *B37*, 1276.
(21) Anderson, L.; Moret, J. *Acta Crystallogr.* **1983**, *C39*, 143.
(22) Pertlik, F. *J. Solid State Chem.* **1987**, *71*, 291.
(23) Feger, C. R.; Kolis, J. W. *Inorg. Chem.* **1998**, *37*, 4046.
(24) Feger, C. R.; Kolis, J. W. *Acta Crystallogr.* **1998**, *C54*, 1055.
(25) Feger, C. R.; Kolis, J. W. *Acta Crystallogr.* **1998**, *C54*, 1217.
(26) Feger, C. R.; Schimek, G. L.; Kolis, J. W. *J. Solid State Chem.* **1999**, *143*, 246.

10.1021/cm0103489 CCC: $20.00
Published on Web 10/10/2001

mented.[27] Both acids and bases have been used as mineralizers to aid in the dissolution of sparingly soluble compounds (oxides) with high melting points.[28,29] At the elevated temperatures (T > 374 °C) and pressures (P > 218 atm) employed, an environment exists where meta-stable compounds may form and, upon slow cooling, produce single crystals. We have utilized a supercritical hydrothermal technique with KOH, Ga_2O_3, and TeO_2 as reagents to synthesize $K_2Te_4O_9{\cdot}3.2H_2O$, $KGaTe_6O_{14}$, and $KGaTe_2O_6{\cdot}1.8H_2O$, and we report here their syntheses, single-crystal structures, and characterization.

Experimental Section

Reagents. Ga_2O_3 (99.99%, Alfa Aesar) and TeO_2 (99+%, Aldrich) were used as received.

Syntheses. For $K_2Te_4O_9{\cdot}3.2H_2O$, 0.059 g (3.71×10^{-4} mol) of TeO_2 were combined with 0.330 mL of 1.5 M (4.95×10^{-4} mol) KOH. For $KGaTe_6O_{14}$, 0.023 g (1.23×10^{-4} mol) of Ga_2O_3 and 0.080 g (5.01×10^{-4} mol) of TeO_2 were combined with 0.348 mL of 0.5 M (1.74×10^{-4} mol) KOH. For $KGaTe_2O_6{\cdot}1.8H_2O$, 0.023 g (1.23×10^{-4} mol) of Ga_2O_3 and 0.080 g (5.01×10^{-4} mol) of TeO_2 were combined with 0.409 mL of 1.5 M (6.14×10^{-4} mol) KOH.

The respective solutions were placed in separate gold tubes (i.d. = 4.7 mm, o.d. = 4.9 mm, and length = 59.0 mm) that were subsequently sealed and introduced into an autoclave (Autoclave Engineers). The autoclave was filled with 56 mL of H_2O (60% fill), closed, and heated at 430 °C for 72 h and cooled slowly at 6 °C h^{-1} to room temperature. At 430 °C, an autogenous pressure of 6250 psi (425 atm) is generated by water. After cooling to room temperature, the autoclave and gold tubes were opened and the products were recovered by filtration. $K_2Te_4O_9{\cdot}3.2H_2O$ was initially synthesized as an impurity phase, formed during the synthesis of $KGaTe_2O_6{\cdot}1.8H_2O$. By adjusting the initial synthetic conditions, we were able to synthesize both materials in phase pure form. For $K_2Te_4O_9{\cdot}3.2H_2O$, $KGaTe_6O_{14}$, and $KGaTe_2O_6{\cdot}1.8H_2O$, colorless crystals, the only product from the reaction, were recovered in 27%, 76%, and 48% yields respectively, based on TeO_2. Powder X-ray diffraction patterns on the synthesized phases are in good agreement with the generated pattern from the single-crystal data (see the Supporting Information).

Crystallographic Determination. The structures of $K_2Te_4O_9{\cdot}3.2H_2O$, $KGaTe_6O_{14}$, and $KGaTe_2O_6{\cdot}1.8H_2O$ were determined by standard crystallographic methods. Room-temperature intensity data were collected on a Siemens SMART diffractometer equipped with a 1K CCD area detector using graphite monochromated Mo Kα radiation. A hemisphere of data was collected using a narrow-frame method with scan widths of 0.30° in omega and an exposure time of 25 s/frame. The first 50 frames were remeasured at the end of the data collection to monitor instrument and crystal stability. The maximum correction applied to the intensities was < 1%. The data were integrated using the Siemens SAINT program,[30] with the intensities corrected for Lorentz, polarization, air absorption, and absorption attributable to the variation in the path length through the detector faceplate. Psi scans were used for the absorption correction on the hemisphere of data. The data were solved and refined using SHELXS-97 and SHELXL-97, respectively.[31,32] All of the atoms were refined with anisotropic thermal parameters and converged for $I > 2\sigma(I)$. All calculations were performed using the WinGX 98 crystallographic software package.[33] Crystallographic data, atomic coordinates and thermal parameters, and selected bond distances for $K_2Te_4O_9{\cdot}3.2H_2O$, $KGaTe_6O_{14}$, and $KGaTe_2O_6{\cdot}1.8H_2O$ are given in Tables 1−7.

Infrared Spectroscopy. Infrared spectra were recorded on a Matteson FTIR 5000 spectrometer in the 400−4000 cm^{-1} range, with the sample pressed between two KBr pellets.

Thermogravimetric Analysis. Thermogravimetric analyses were carried out on a TGA 2950 thermogravimetric

Table 1. Crystallographic Data for $K_2Te_4O_9{\cdot}3.2H_2O$, $KGaTe_6O_{14}$, and $KGaTe_2O_6{\cdot}1.8H_2O$

chem formula	$Te_4K_2O_{12.2}H_{6.4}$	Te_6GaKO_{14}	$Te_2GaKO_{7.8}H_{3.6}$
fw	790.20	1098.42	492.42
space group	*P*1 (No. 1)	*Pa*-3 (No. 205)	*P*-1 (No. 2)
a, Å	7.5046 (5)	10.9267 (3)	8.8361 (6)
b, Å	10.7097 (8)	10.9267 (3)	9.1648 (6)
c, Å	10.7159 (8)	10.9267 (3)	9.9531 (7)
α, deg	60.849 (1)	90	115.395 (1)
β, deg	69.918 (1)	90	93.973 (1)
γ, deg	85.968 (1)	90	116.011 (1)
V, Å^3	701.49 (9)	1304.57 (6)	620.63 (7)
Z	2	4	3
ρ, g/cm^3	3.81	5.59	3.95
μ, cm^{-1}	88.86	156.6	107.5
R(F)[a]	0.032	0.017	0.027
R_w(F)[b]	0.086	0.046	0.063

[a] $R = \sum||F_o| - |F_c||/\sum|F_o|$. [b] $R_w = [\sum w(|F_o^2| - |F_c^2|)^2/\sum w(F_o^2)^2]^{1/2}$.

Table 2. Atomic Coordinates for $K_2Te_4O_9{\cdot}3.2H_2O$

atom	*x*	*y*	*z*	*U*(eq) (Å^2)[a]
Te(1)	0.53829(10)	0.84045(7)	0.81729(7)	0.01693(19)
Te(2)	0.50156(10)	0.52144(8)	0.80781(9)	0.01812(19)
Te(3)	0.46468(10)	0.82307(8)	0.48946(8)	0.01745(18)
Te(4)	0.49029(10)	0.80979(8)	0.16778(8)	0.01788(19)
Te(5)	0.45501(10)	0.48044(8)	0.19661(9)	0.01793(19)
Te(6)	0.50093(10)	0.17882(9)	0.51519(9)	0.01800(18)
Te(7)	0.47173(10)	0.18742(8)	0.84096(8)	0.01778(19)
Te(8)	0.46026(10)	0.16005(7)	0.18367(7)	0.01656(19)
K(1)	0.2069(4)	0.4741(3)	0.5760(3)	0.0265(5)
K(2)	0.8281(4)	0.5305(3)	0.3849(4)	0.0413(7)
K(3)	0.0138(5)	0.6268(4)	0.9095(5)	0.0605(11)
K(4)	0.9729(4)	0.0755(4)	0.8580(4)	0.0459(8)
O(1)	0.3812(11)	0.6694(9)	0.8902(10)	0.0235(17)
O(2)	0.4005(10)	0.9566(8)	0.6902(9)	0.0216(16)
O(3)	0.3861(10)	0.8655(9)	0.9836(9)	0.0207(16)
O(4)	0.3078(11)	0.3812(9)	0.9710(9)	0.0250(18)
O(5)	0.3617(11)	0.6103(9)	0.6760(9)	0.0232(17)
O(6)	0.5758(12)	0.3830(9)	0.7150(9)	0.0271(19)
O(7)	0.6669(11)	0.8102(9)	0.5505(9)	0.0226(17)
O(8)	0.5565(13)	0.7350(9)	0.3637(9	0.028(2)
O(9)	0.6046(11)	0.0259(9)	0.2941(9)	0.0231(16)
O(10)	0.3024(11)	0.9061(9)	0.2358(10)	0.0251(18)
O(11)	0.3389(12)	0.6304(9)	0.2647(9)	0.0267(18)
O(12)	0.6524(11)	0.6193(9)	0.0483(10)	0.0265(19)
O(13)	0.5445(13)	0.4029(10)	0.3623(10)	0.0284(19)
O(14)	0.6077(11)	0.3255(8)	0.1330(10)	0.0253(18)
O(15)	0.3128(11)	0.1637(9)	0.4436(10)	0.0239(17)
O(16)	0.3546(11)	0.2209(9)	0.6695(9)	0.0242(18)
O(17)	0.6704(11)	0.1137(9)	0.7503(9)	0.0229(17)
O(18)	0.6083(11)	0.1621(10)	−0.0048(9)	0.0258(18)
O(19)[b]	−0.0135(15)	0.3516(14)	0.8788(12)	0.036(3)
O(20)[b]	0.0000(14)	0.2933(11)	0.5357(12)	0.024(2)
O(21)[b]	0.9907(15)	0.6883(11)	0.4790(14)	0.038(4)
O(22)[b]	0.9969(14)	0.7644(14)	0.0934(13)	0.039(3)
O(23)[b]	−0.040(2)	0.3507(18)	0.2056(13)	0.058(4)
O(24)[b]	0.0244(14)	0.9070(12)	0.7083(14)	0.039(3)
O(25)[b]	0.9941(17)	0.0170(17)	0.1297(15)	0.048(4)
O(26)[b]	0.9453(17)	0.0336(14)	0.4381(15)	0.045(3)

[a] *U*(eq) is defined as one-third of the trace of the orthogonalized U_{ij} tensor. [b] Constrained with an occupancy of 0.8.

(27) Rabenau, A. *Angew. Chem., Int. Ed. Engl.* **1985**, *24*, 1026.
(28) Laudise, R. A.; Ballman, A. A. *J. Am. Chem. Soc.* **1958**, *80*, 2655.
(29) Laudise, R. A. *J. Am. Chem. Soc.* **1958**, *81*, 562.
(30) *SAINT*; Version 4.05; Siemens Analytical X-ray Systems, Inc.: Madison, WI, 1995.
(31) Sheldrick, G. M. *SHELXS-97 − A program for automatic solution of crystal structures.*; University of Goettingen: Goettingen, Germany, 1997.
(32) Sheldrick, G. M. *SHELXL-97 − A program for crystal structure refinement.*; University of Goettingen: Goettingen, Germany, 1987.
(33) Farrugia, L. J. *WinGX: An integrated system of publically available windows programs for the solution, refinement, and analysis of single-crystal X-ray diffraction data.*: University of Glasgow: Glasgow, Scotland, 1998.

Table 3. Atomic Coordinates for $KGaTe_6O_{14}$

atom	*x*	*y*	*z*	*U*(eq) (Å^2)[a]
Te	0.27159(3)	0.50895(3)	0.26507(3)	0.01031(14)
Ga	0.5000	0.5000	0.5000	0.0083(2)
K	0.5000	0.5000	0.0000	0.0157(5)
O(1)	0.3753(3)	0.3892(3)	0.1936(3)	0.0130(6)
O(2)	0.3744(3)	0.5666(3)	0.3866(3)	0.0131(6)
O(3)	0.3528(3)	0.6472(3)	0.1472(3)	0.0126(11)

[a] *U*(eq) is defined as one-third of the trace of the orthogonalized U_{ij} tensor.

Table 4. Atomic Coordinates for $KGaTe_2O_6 \cdot 1.8H_2O$

atom	*x*	*y*	*z*	*U*(eq) (Å^2)[a]
Te(1)	0.93500(4)	−0.07096(4)	0.80018(4)	0.01183(10)
Te(2)	0.39160(4)	−0.67654(4)	0.78633(4)	0.01164(10)
Te(3)	0.96851(4)	−0.64288(4)	0.78448(4)	0.01165(10)
Ga(1)	0.0000	0.0000	0.5000	0.01107(16)
Ga(2)	0.80418(7)	−0.37648(8)	0.90870(6)	0.01102(13)
K(1)	0.31013(18)	−0.1291(2)	0.76858(16)	0.0291(3)
K(2)	0.5000	−0.5000	0.5000	0.0313(4)
O(1)	0.1473(5)	0.1119(5)	0.9704(4)	0.0149(7)
O(2)	0.3137(5)	−0.5483(5)	0.9426(4)	0.0162(7)
O(3)	0.5668(5)	−0.4641(5)	0.7881(4)	0.0140(7)
O(4)	0.8618(5)	−0.8941(5)	0.6200(4)	0.0166(7)
O(5)	0.9702(5)	−0.6977(5)	0.9487(4)	0.0157(7)
O(6)	0.7599(5)	−0.6336(5)	0.7780(4)	0.0146(7)
O(7)	0.9321(5)	−0.2866(5)	0.7790(4)	0.0138(7)
O(8)	0.2192(5)	−0.7443(5)	0.6149(4)	0.0155(7)
O(9)	0.0622(5)	−0.0531(5)	0.6582(4)	0.0170(8)
O(10)[b]	0.1812(7)	−0.4924(7)	0.5558(5)	0.0299(11)
O(11)[b]	0.3741(7)	−0.1875(7)	0.0065(6)	0.0308(11)
O(12)[b]	0.4982(6)	−0.1544(7)	0.5510(6)	0.0317(11)

[a] *U*(eq) is defined as one-third of the trace of the orthogonalized U_{ij} tensor. [b] Constrained with an occupancy of 0.9.

Table 5. Selected Bond Distances (Å) for $K_2Te_4O_9 \cdot 3.2H_2O$

Te(1)−O(1)	1.906(9)	Te(5)−O(11)	2.092(9)
Te(1)−O(2)	1.899(7)	Te(5)−O(12)	1.823(8)
Te(1)−O(3)	1.891(7)	Te(5)−O(13)	1.897(8)
Te(2)−O(1)	2.172(9)	Te(5)−O(14)	2.198(9)
Te(2)−O(4)	1.852(7)	Te(6)−O(2)	2.164(7)
Te(2)−O(5)	1.890(8)	Te(6)−O(13)[b]	2.112(9)
Te(2)−O(6)	2.106(8)	Te(6)−O(15)	1.872(9)
Te(3)−O(5)	2.129(8)	Te(6)−O(16)	1.885(8)
Te(3)−O(7)	1.820(8)	Te(7)−O(6)[b]	1.890(8)
Te(3)−O(8)	1.921(8)	Te(7)−O(16)	2.168(9)
Te(3)−O(9)	2.141(8)	Te(7)−O(17)	1.838(8)
Te(4)−O(3)[a]	2.170(9)	Te(7)−O(18)[c]	2.132(9)
Te(4)−O(8)	2.078(8)	Te(8)−O(9)	1.908(8)
Te(4)−O(10)	1.846(8)	Te(8)−O(14)[b]	1.893(8)
Te(4)−O(11)	1.901(9)	Te(8)−O(18)	1.932(8)

[a] Symmetry transformations used to generate equivalent atoms: $x, y, z - 1$. [b] Symmetry transformations used to generate equivalent atoms: $x, y + 1, z$. [c] Symmetry transformations used to generate equivalent atoms: $x, y, z + 1$.

Table 6. Selected Bond Distances (Å) for $KGaTe_6O_{14}$

Te−O(1)	1.899(3)
Te−O(1)[a]	2.168(3)
Te−O(2)	1.851(3)
Te−O(3)	2.1744(10)
Ga−O(2)	1.986(3) × 6

[a] Symmetry transformations used to generate equivalent atoms: *z*, *x*, *y*.

analyzer (TA Instruments). The samples were contained within platinum crucibles and heated at a rate of 5 °C min^{-1} from room temperature to 600 °C in static air.

Ion-Exchange Experiments. Ion-exchange reactions were performed by stirring ca. 100 mg of polycrystalline $KGaTe_2O_6 \cdot 1.8H_2O$ in 5 mL of 1 M aqueous solution of the following metal salts: $LiNO_3$, $NaNO_3$, $RbNO_3$, and $CsNO_3$. The reactions were performed at room temperature for 24 h and then at 50 °C for 72 h. The ion-exchanged products were recovered by filtration, washed with excess H_2O, and dried in air for 1 day. The extent of the ion exchange was investigated by inductively coupled plasma analysis.

Table 7. Selected Bond Distances (Å) for $KGaTe_2O_6 \cdot 1.8H_2O$

Te(1)−O(1)	1.888(4)	Ga(1)−O(8)	1.991(4)
Te(1)−O(7)	1.884(3)	Ga(1)−O(8)[a]	1.991(4)
Te(1)−O(9)	1.882(3)	Ga(1)−O(9)[b]	1.947(3)
Te(2)−O(2)	1.888(3)	Ga(1)−O(9)[c]	1.947(3)
Te(2)−O(3)	1.874(3)	Ga(2)−O(1)[d]	2.006(4)
Te(2)−O(8)	1.875(3)	Ga(2)−O(2)[e]	2.052(3)
Te(3)−O(4)	1.876(4)	Ga(2)−O(3)[f]	1.958(4)
Te(3)−O(5)	1.906(3)	Ga(2)−O(5)[e]	2.010(4)
Te(3)−O(6)	1.881(3)	Ga(2)−O(6)	1.972(4)
Ga(1)−O(4)[a]	2.026(3)	Ga(2)−O(7)	1.980(3)
Ga(1)−O(4)	2.026(3)		

[a] Symmetry transformations used to generate equivalent atoms: $-x + 2, -y - 2, -z + 1$. [b] Symmetry transformations used to generate equivalent atoms: $-x + 2, -y - 1, -z + 1$. [c] Symmetry transformations used to generate equivalent atoms: $x, y - 1, z$. [d] Symmetry transformations used to generate equivalent atoms: $-x + 2, -y, -z + 2$. [e] Symmetry transformations used to generate equivalent atoms: $-x + 2, -y - 1, -z + 2$. [f] Symmetry transformations used to generate equivalent atoms: $x - 1, y, z$.

Inductively Coupled Plasma Analysis. The exchanged solids were dissolved in ca. 1 M HNO_3 and diluted with H_2O. The final concentration of the alkali metal ions in solution was measured using an Atom Scan 25 (Thermo Jarrell Ash) ICP-AES spectrometer.

Results and Discussion

$K_2Te_4O_9 \cdot 3.2H_2O$ has a layered structure consisting of tellurium(IV) oxide polyhedra that share corners. The Te^{4+} cations are bonded to either three or four oxygen atoms, resulting in a highly asymmetric coordination environment attributable to the nonbonded electron pair (see Figure 1). The connectivity of the tellurium polyhedra within the layer generates a star motif (see Figure 2). In connectivity terms, the entire layer can be described as consisting of $[TeO_{3/2}]^+$ cations linked to $[TeO_{3/2}O_{1/1}]^-$ anions that form a $\{[TeO_{3/2}]^+3\text{-}[TeO_{3/2}O_{1/1}]^-\}^{2-}$ sheet. The anionic layers are separated by K^+ cations and occluded H_2O molecules. Bond valence calculations on $K_2Te_4O_9 \cdot 3.2H_2O$ resulted in values ranging from 3.58 to 4.18 for Te^{4+},[34,35] with the distances for the Te^{4+}-O bonds ranging from 1.829(7) to 2.203(8) Å. Crystallographers and others will note that for space group *P*1 (No. 1) $Z = 2$ is extremely rare and usually indicates higher (centrosymmetric) symmetry.[36] Powder second-harmonic generation measurements, using 1064 nm radiation, on $K_2Te_4O_9 \cdot 3.2H_2O$ did reveal a faint green signal with an intensity similar to SiO_2. Although consistent with the chosen space group, the possibility that the signal was attributable to surface or other spurious effects could not be ignored. Therefore, we attempted to confirm the noncentrosymmetry by closely examining the structure. Using the PLATON suite of crystallographic programs,[37] we determined that the anionic tellurium-oxide layer *does possess* a center of symmetry at (0, 0, 0). However, the inversion symmetry is broken upon the incorporation of the K^+

(34) Brown, I. D.; Altermatt, D. *Acta Crystallogr.* **1985**, *B41*, 244.
(35) Brese, N. E.; O'Keeffe, M. *Acta Crystallogr.* **1991**, *B47*, 192.
(36) Marsh, R. E. *Acta Crystallogr.* **1995**, *B51*, 897.
(37) Spek, A. L. *Platon: A Multi-purpose Crystallographic Tool*, Utrecht University; Utrecht, The Netherlands, 2001.

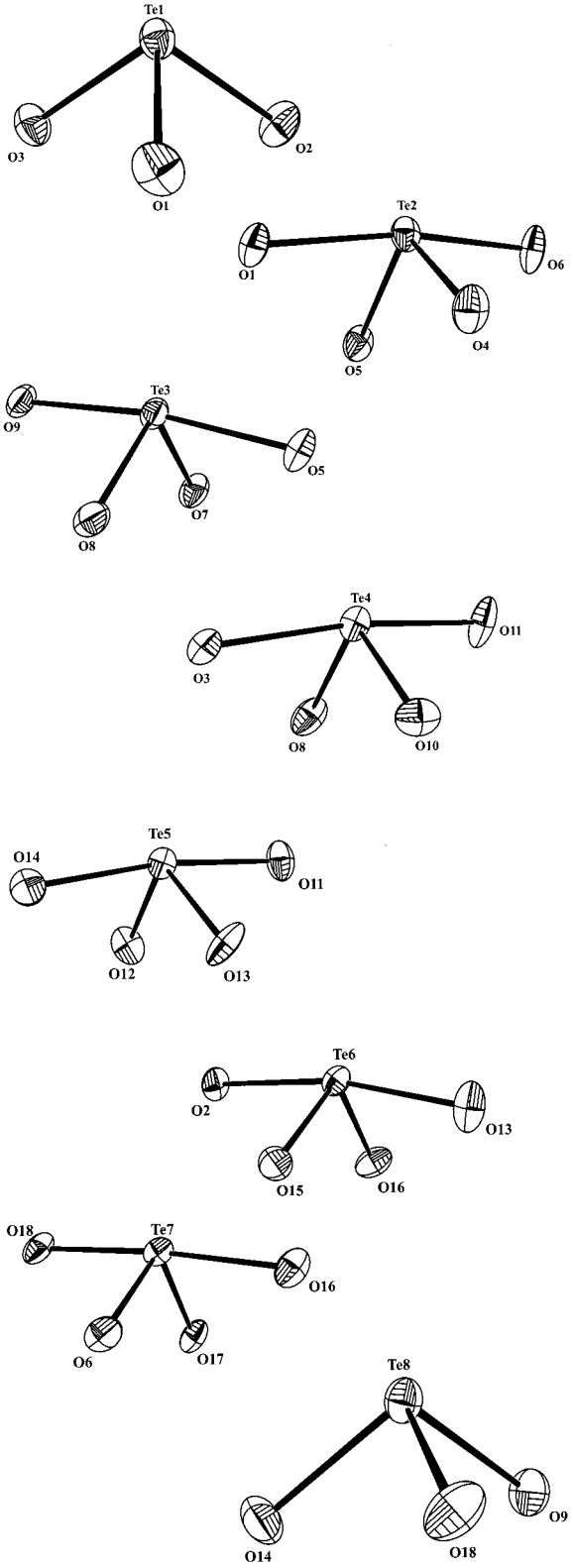

Figure 1. ORTEP (50% probability ellipsoids) for Te(1)−Te(8) in $K_2Te_4O_9{\cdot}3.2H_2O$.

cations. Zwanziger et al. have previously reported $K_2Te_4O_9$.[17] Their structure, although not isostructural to our compound, shows many similarities. Both $K_2Te_4O_9$ and $K_2Te_4O_9{\cdot}3.2H_2O$ have layered structures, but the former contains several singly bonded oxygen atoms as well as a twelve-member ring of tellurite polyhedra.

$KGaTe_6O_{14}$ has a three-dimensional structure consisting of distorted TeO_4 polyhedra that are linked to

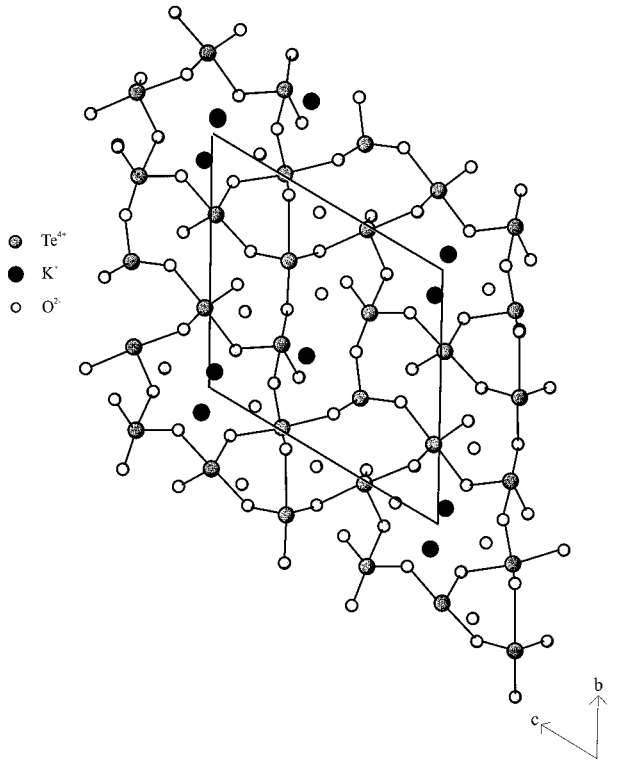

Figure 2. Ball-and-stick representation of one layer of $K_2Te_4O_9{\cdot}3.2H_2O$. Note the "star motif" of the six Te^{4+} cations.

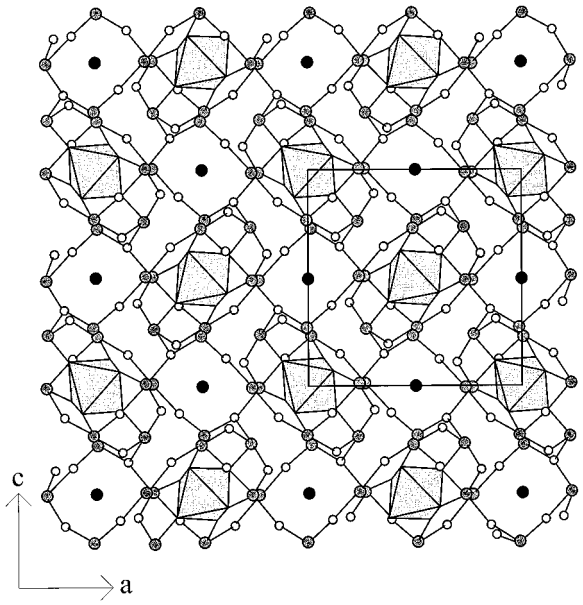

Figure 3. Ball-and-stick (Te^{4+}) and polyhedral (Ga^{3+}) of $KGaTe_6O_{14}$.

GaO_6 octahedral through oxygen atoms (see Figure 3). Each gallium octahedron is surrounded by six tellurium polyhedra, whereas each tellurium polyhedra is connected to an additional two tellurium polyhedra and one gallium octahedron. Thus, in connectivity terms, the material can be described as a three-dimensional framework of $\{6[TeO_{3/2}O_{1/3}]^{+1/3}[GaO_{6/2}]^{3-}\}^-$. Charge neutrality is maintained by the K^+ cation. Bond valence calculations on $KGaTe_6O_{14}$ resulted in values of 3.82 and 2.99 for Te^{4+} and Ga^{3+}, respectively.[34,35] The distances for the Te^{4+}−O bonds range from 1.851(3) to 2.174(1) Å, whereas all six Ga−O bonds are 1.986(3) Å. Although

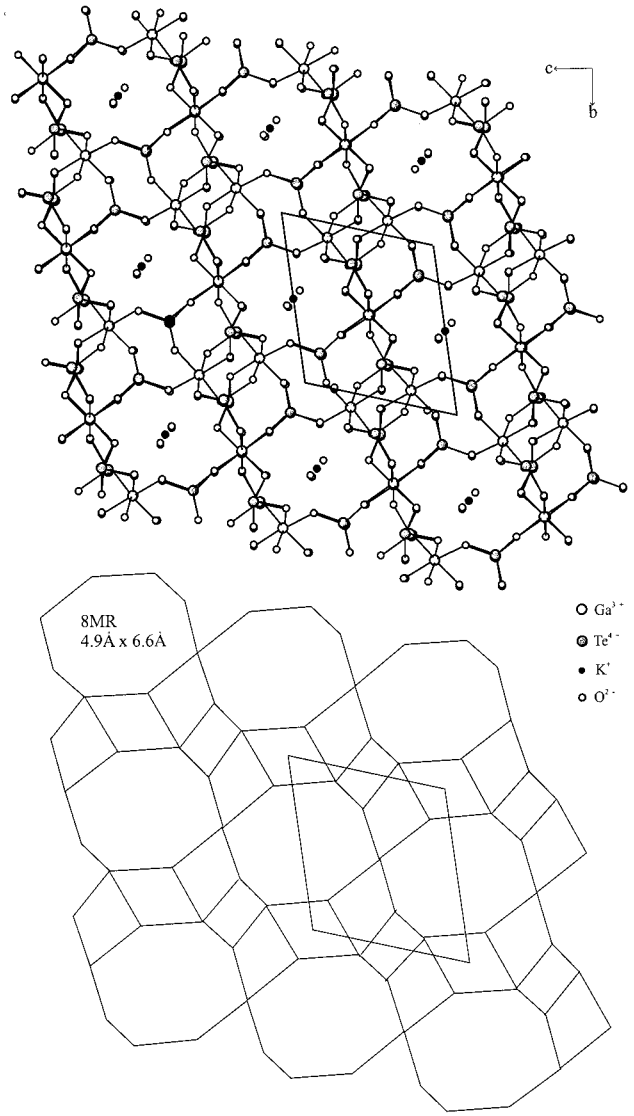

Figure 4. Ball-and-stick and wire representation of $KGaTe_2O_6 \cdot 1.8H_2O$ showing the 8-MR channels along the [100] direction.

$KGaTe_6O_{14}$ contains a substantial number of distorted tellurite polyhedra, the material has a densely packed crystal structure. In fact, the nonbonded electron pair on the Te^{4+} cations point toward the K^+.

$KGaTe_2O_6 \cdot 1.8H_2O$ also has a three-dimensional structure consisting of distorted TeO_3 polyhedra linked to GaO_6 octahedra through the oxygen atoms. In connectivity terms, the structure can be described as consisting of $[TeO_{3/2}]^+$ cations linked to $[GaO_{6/2}]^{3-}$ anions that form a $\{2[TeO_{3/2}]^+[GaO_{6/2}]^{3-}\}^-$ network. Charge neutrality is maintained through the K^+ cation. Bond valence calculations on $KGaTe_2O_6 \cdot 1.8H_2O$ resulted in values ranging from 3.83 to 3.90 for Te^{4+} and 2.92 to 2.98 for Ga^{3+}.[34,35] The distances for the $Te^{4+}-O$ and $Ga^{3+}-O$ bonds range from 1.873(4) to 1.906(4) Å and 1.948(4) to 2.054(4) Å, respectively. $KGaTe_2O_6 \cdot 1.8H_2O$ has an open-framework structure consisting of three, mutually perpendicular, eight-membered rings (8-MR) along the [100], [010], and [001] directions (see Figures 4−6). Each side of the ring is defined by a line drawn between two adjacent metal atoms. Each channel consists of four $[TeO_{3/2}]^+$ cations and four $[GaO_{6/2}]^{3-}$ anions that alternate around the ring. The channels are very similar in size, taking into account the atomic radii of oxygen,[38] with dimensions of 4.9 × 6.6 Å [100], 4.5 × 6.7 Å [010], and 4.4 × 6.7 Å [001]. Within the rings are the K^+ cations and occluded H_2O molecules.

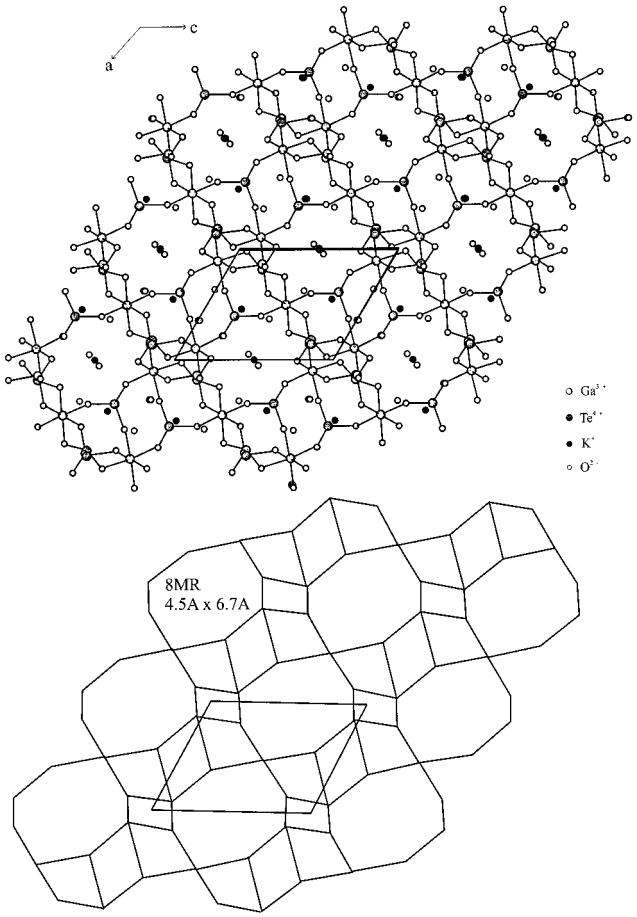

Figure 5. Ball-and-stick and wire representation of $KGaTe_2O_6 \cdot 1.8H_2O$ showing the 8-MR channels along the [010] direction.

Compared to other materials, $KGaTe_2O_6 \cdot 1.8H_2O$ has a moderately open-framework structure. Two parameters that are generally used to quantify the "openness" of a structure are the framework density and the amount of void space. The framework density is defined as the number of metal atoms for a volume of 1000 $Å^3$. For $KGaTe_2O_6 \cdot 1.8H_2O$, the framework density is 14.6 that compares well to faujasite (12.7) and cloverite (11.1). However, care must be taken when comparing framework densities of zeolitic and other completely tetrahedrally coordinated structures to structures containing octahedral and other coordination polyhedra. The amount of void space can also be calculated by removing all of the nonframework atoms, K^+ and the occluded H_2O molecules and using the CALC SOLV command in PLATON.[37] For $KGaTe_2O_6 \cdot 1.8H_2O$, the amount of void space is 36%, whereas for faujasite and cloverite, the analogous values are 84% and 60%, respectively. When the K^+ cations and the H_2O molecules are included in the calculation for $KGaTe_2O_6 \cdot 1.8H_2O$, the void space becomes zero.

Infrared Spectroscopy. The infrared spectra of the materials revealed Te−O and Ga−O stretches between 749 and 792 cm^{-1} and at ca. 660 and 450 cm^{-1}, respectively. In addition, Te−O−Te and Te−O−Ga

(38) Shannon, R. D. *Acta Crystallogr.* **1976**, *A32*, 751.

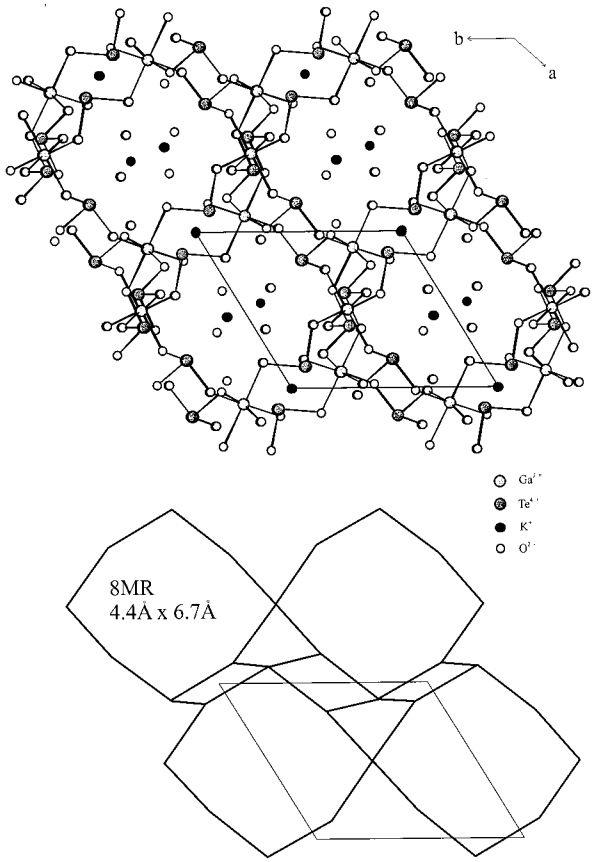

Figure 6. Ball-and-stick and wire representation of $KGaTe_2O_6 \cdot 1.8H_2O$ showing the 8-MR channels along the [001] direction.

Table 8. Infrared Vibrations (cm^{-1}) for $K_2Te_4O_9 \cdot 3.2H_2O$, $KGaTe_6O_{14}$, and $KGaTe_2O_6 \cdot 1.8H_2O$

	Te−O	Ga−O	Te−O−Te	Te−O−Ga
$K_2Te_4O_9 \cdot 3.2H_2O$	749		667	
			623	
			474	
$KGaTe_6O_{14}$	792	667	667	690
	770	441	415	593
	776			
$KGaTe_2O_6 \cdot 1.8H_2O$	770	660		704
		448		494

bends were observed between 415 and 704 cm^{-1} (see Table 8). Finally, for $K_2Te_4O_9 \cdot 3.2H_2O$ and $KGaTe_2O_6 \cdot 1.8H_2O$, vibrations attributable to H_2O were observed at ca. 1650 and 3420 cm^{-1}, respectively. The assignments are consistent with those previously reported.[39−41]

Thermogravimetric Analysis (TGA). The thermal behavior of $K_2Te_4O_9 \cdot 3.2H_2O$ and $KGaTe_2O_6 \cdot 1.8H_2O$ were investigated using thermogravimetric analysis. Both $K_2Te_4O_9 \cdot 3.2H_2O$ and $KGaTe_2O_6 \cdot 1.8H_2O$ show a weight loss of 7.30% and 6.60% between room temperature and 250°C, respectively, that is attributed to the loss of the occluded water molecules from the materials. Only the loss of occluded water from $KGaTe_2O_6 \cdot 1.8H_2O$ is fully reversible; if the material is heated to 200 °C then cooled back to room temperature and allowed to stand in atmospheric air, complete rehydration occurs within a few hours.

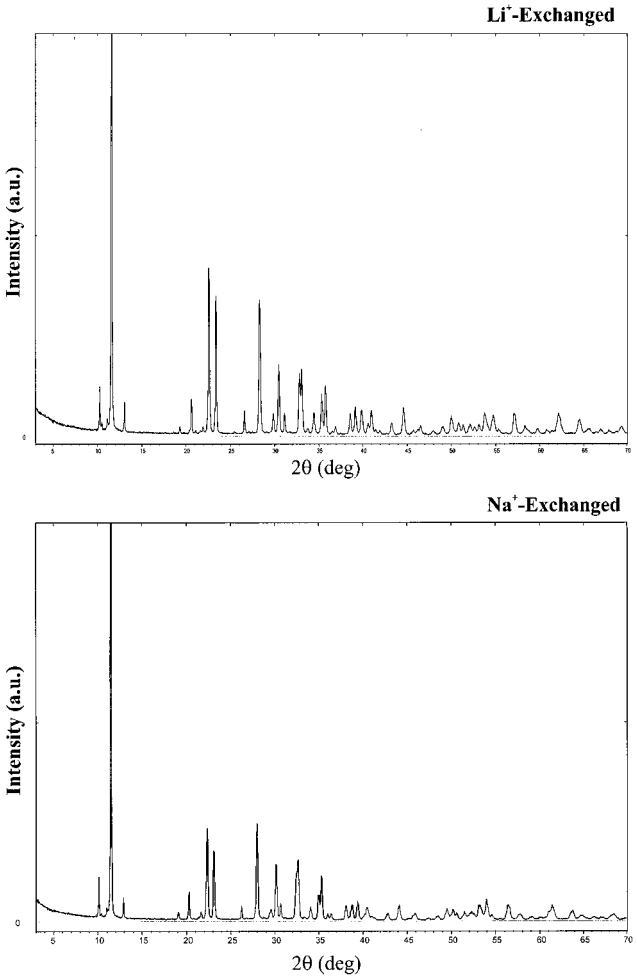

Figure 7. Powder X-ray diffraction patterns (Cu Kα radiation) of the product of the ion exchange of $KGaTe_2O_6 \cdot 1.8H_2O$ with Li^+ (top) and Na^+ (bottom) cations. Both patterns can be indexed on a rhombohedral cell with $a = b \sim 9.29$ Å and $c \sim 26.22$ Å.

Ion-Exchange Experiments. The open-framework nature of $KGaTe_2O_6 \cdot 1.8H_2O$ suggested the material may be able to undergo ion-exchange reactions in which the K^+ cation is replaced by other cationic species. Our experiments revealed that $KGaTe_2O_6 \cdot 1.8H_2O$ displays robust ion-exchange behavior. It was possible to completely exchange the K^+ cation for Li^+ and Na^+ by stirring a suspension of the host material in an ∼1 M solution of the appropriate metal nitrate salts for 1 day at room temperature and then an additional 3 days at 50 °C. Using a similar technique, we were unable to exchange the K^+ for Rb^+ or Cs^+. With both the Li^+- and Na^+-exchanged materials, the powder X-ray diffraction patterns revealed a highly crystalline material (see the Supporting Information). In addition the exchanged materials have very similar XRD patterns (see Figure 7) and may be indexed on a rhombohedral cell with $a = b \sim 9.29$ Å and $c \sim 26.22$ Å. A full ab initio structural determination using powder data is in progress to determine the crystal structure of these phases. The powder XRD patterns of the Li^+- and Na^+-exchanged materials does not match any known phases, including the recently reported $NaGaTe_2O_6 \cdot 2.4H_2O$,[15] suggesting that the ion exchange of $KGaTe_2O_6 \cdot 1.8H_2O$ provides a facile route for the low-temperature synthesis of new alkali-metal gallium tellurites. Work is underway to

(39) Alonso, J. A.; Castro, A.; Jerez, A.; Pico, C.; Viega, M. L. *J. Chem. Soc., Dalton. Trans.* **1985**, 2225.
(40) Cabello, C. I.; Botto, I. L.; Baran, E. J. *Z. Anorg. Allg. Chem.* **1985**, *523*, 234.
(41) Balraj, V.; Vidyasagar, K. *Inorg. Chem.* **1999**, *38*, 3458.

confirm the phase purity of these materials and to determine their structures.

Conclusion/Summary

In summary, we have reported a single-step route to the exclusive synthesis of new tellurites, one of which, $KGaTe_2O_6 \cdot 1.8H_2O$, represents a novel open-framework material. Of particular interest is the variable coordination of the Te^{4+} cation. The flexibility of the Te^{4+} coordination environment, in combination with octahedral or tetrahedral moieties offers great promise for the synthesis of materials with extremely large channels or perhaps cages. We are continuing to explore the synthesis of new tellurites as well as investigate the incorporation of other cations with stereoactive lone pairs into open-framework structures.

Acknowledgment. We acknowledge Dr. James Korp for technical assistance with the crystallography, and Dr. Anne McGuire for assistance with the ICP analysis. We thank the Robert A. Welch Foundation for support. This work was supported in part by the MRSEC program of the National Science Foundation under Award Number DMR-9632667 and by the State of Texas through the Texas Center for Superconductivity at the University of Houston. This work was also supported by the NSF-Career Program through DMR-0092054.

Supporting Information Available: Powder X-ray diffraction patterns (calculated and experimental), ORTEP diagrams (50% probability ellipsoids) for $K_2Te_4O_9 \cdot 3.2H_2O$, $KGaTe_6O_{14}$, and $KGaTe_2O_6 \cdot 1.8H_2O$, and the powder X-ray diffraction patterns for the ion-exchanged materials are available (PDF). A file of X-ray crystallographic data is also available (CIF). This material is available free of charge via the Internet at http://pubs.acs.org.

CM0103489